

Atrophy and structural variability of the upper cervical cord in early multiple sclerosis

Viola Biberacher, Christine C Boucard, Paul Schmidt, Christina Engl, Dorothea Buck, Achim Berthele, Muna-Miriam Hoshi, Claus Zimmer, Bernhard Hemmer and Mark Mühlau

Multiple Sclerosis Journal

2015, Vol. 21(7) 875–884

DOI: 10.1177/
1352458514546514

© The Author(s), 2014.
Reprints and permissions:
[http://www.sagepub.co.uk/
journalsPermissions.nav](http://www.sagepub.co.uk/journalsPermissions.nav)

Abstract

Background: Despite agreement about spinal cord atrophy in progressive forms of multiple sclerosis (MS), data on clinically isolated syndrome (CIS) and relapsing–remitting MS (RRMS) are conflicting.

Objective: To determine the onset of spinal cord atrophy in the disease course of MS.

Methods: Structural brain magnetic resonance imaging (MRI) was acquired from 267 patients with CIS (85) or RRMS (182) and 64 healthy controls (HCs). The upper cervical cord cross-sectional area (UCCA) was determined at the level of C2/C3 by a segmentation tool and adjusted for focal MS lesions. The coefficient of variation (CV) was calculated from all measurements between C2/C3 and 13 mm above as a measure of structural variability.

Results: Compared to HCs ($76.1 \pm 6.9 \text{ mm}^2$), UCCA was significantly reduced in CIS patients ($73.5 \pm 5.8 \text{ mm}^2$, $p=0.018$) and RRMS patients ($72.4 \pm 7.0 \text{ mm}^2$, $p<0.001$). Structural variability was higher in patients than in HCs, particularly but not exclusively in case of focal lesions (mean CV HCs/patients without/with lesions: 2.13%/2.55%/3.32%, all p -values <0.007). UCCA and CV correlated with Expanded Disability Status Scale (EDSS) scores ($r = -0.131/0.192$, $p=0.044/<0.001$) and disease duration ($r = -0.134/0.300$, $p=0.039/<0.001$). CV additionally correlated with hand and arm function ($r=0.180$, $p=0.014$).

Conclusion: In MS, cervical cord atrophy already occurs in CIS. In early stages, structural variability may be a more meaningful marker of spinal cord pathology than atrophy.

Keywords: Cervical cord, clinically isolated syndrome, relapsing–remitting multiple sclerosis, magnetic resonance imaging

Date received: 12 February 2014; accepted: 21 July 2014

Introduction

To date, imaging markers have been insufficient to explain the clinical heterogeneity of multiple sclerosis (MS). One explanation thereof might be the disregard of spinal cord pathology which is more strongly correlated with some aspects of clinical disability than brain imaging parameters. Hence, spinal cord measurements have been proposed to monitor disease progression and response to disease modifying treatment.^{1–4}

Numerous studies have demonstrated spinal cord atrophy in progressive forms of MS,^{2,4–8} while studies on clinically isolated syndrome (CIS) and relapsing–remitting MS (RRMS) have shown inconsistent results.^{2,3,8–15} Pooling these results (Figure 1(a)) in a meta-analysis,^{16–18} we found no clear indication of upper

cervical cord (UCC) atrophy in RRMS. In CIS, our meta-analysis yielded the unexpected finding of significant UCC decrease in one study and significant UCC increase in another. Since we and others^{19,20} had made the observation that, at least in single cases, focal lesions can cause both swelling and shrinking (see Figure 1(b)), we first tested the hypothesis that focal lesions exert a substantial influence on spinal cord measurements at the group level. Accounting for focal MS lesions as potential confounder, we next aimed to determine the onset of spinal cord atrophy by studying a large cohort of healthy controls (HCs) and patients with CIS or RRMS. Finally, we investigated whether measures of UCC pathology yield information regarding the heterogeneity of MS in addition to measures of brain pathology, which would make them promising candidates for clinical practice and research.

Correspondence to:
Viola Biberacher
Department of Neurology,
Technische Universität
München, Ismaningerstr. 22,
D-81675 Munich, Germany.
biberacher@lrz.tum.de

Dorothea Buck
Achim Berthele
Muna-Miriam Hoshi
Department of Neurology,
Technische Universität
München, Germany

Viola Biberacher
Christine C Boucard
Christina Engl
Technische Universität
München, Germany/
TUM–Neuroimaging Center,
Technische Universität
München, Germany

Paul Schmidt
Technische Universität
München, Germany/
TUM–Neuroimaging Center,
Technische Universität
München, Germany/
Ludwig-Maximilians-
University München,
Germany

Claus Zimmer
Technische Universität
München, Germany

Bernhard Hemmer
Technische Universität
München, Germany/
Munich Cluster for Systems
Neurology (SyNergy),
Germany

Mark Mühlau
Technische Universität
München, Germany/
TUM–Neuroimaging Center,
Technische Universität
München, Germany/
Munich Cluster for Systems
Neurology (SyNergy),
Germany

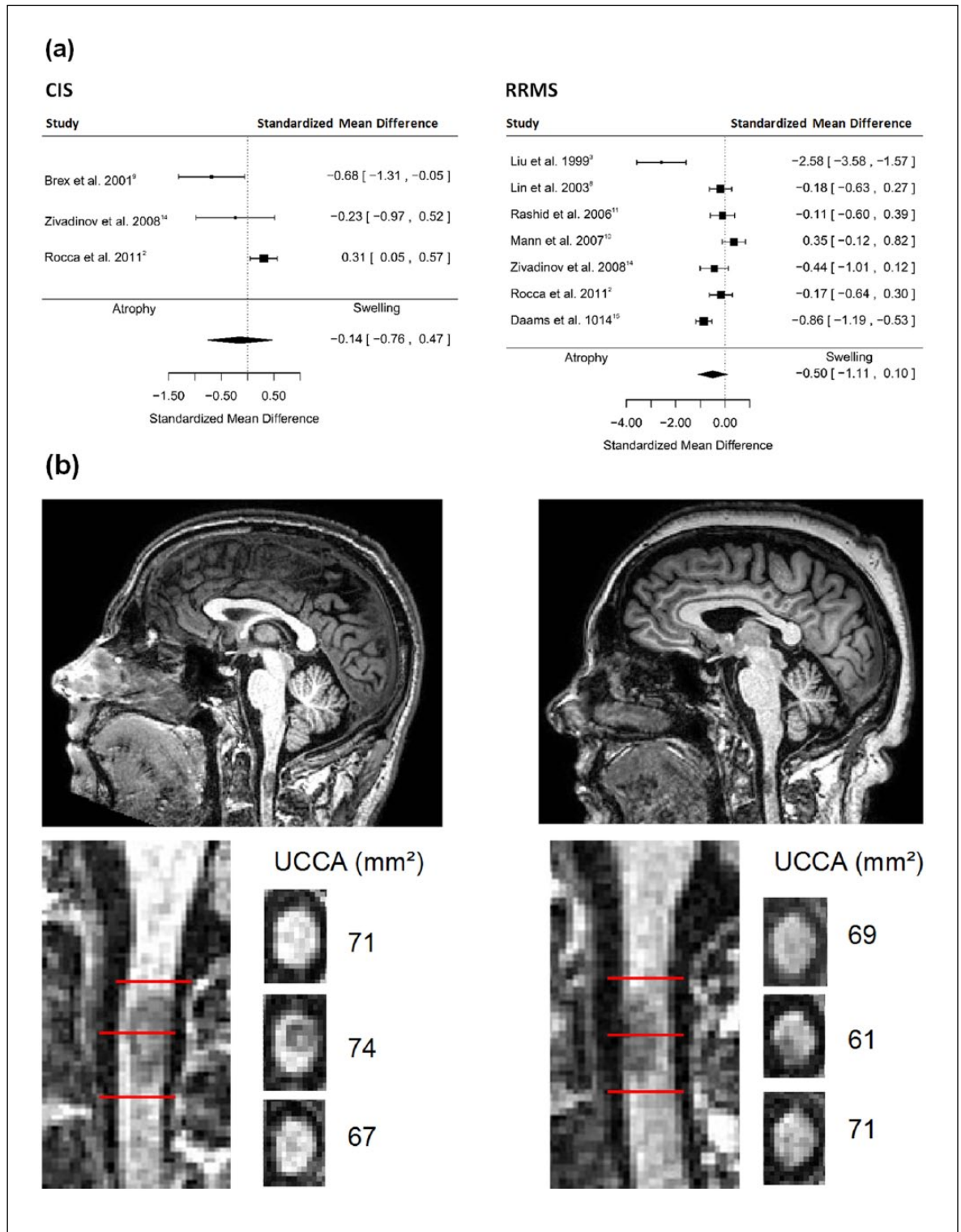


Figure 1. Upper cervical cord in early multiple sclerosis (MS). (a) Meta-analysis of previous studies on the upper cervical cord in early MS: left, clinically isolated syndrome (CIS); right, relapsing–remitting MS (RRMS). (b) Influence of focal lesions in individual patients. The influence of focal lesions on upper cervical cord cross-sectional area (UCCA) is illustrated by two of our examples; one causing local swelling (left) and one causing local shrinking (right). One sagittal and three different axial sections (below, across and above the lesion) and the corresponding UCCA are depicted in each case.

Materials and methods

Meta-analysis

We searched the databases Pubmed, Google Scholar and Cited Reference Search in Web of Science for magnetic resonance imaging (MRI) studies on the cervical cord in CIS and RRMS. The included studies had to provide planimetric or volumetric measurements of the whole cervical cord area in patients with CIS and/or RRMS as well as HCs. Studies overlapping with included datasets were excluded.^{12,13} Sample sizes, means and standard deviations of controls and patients were assembled from all studies and used to calculate standardized mean differences and their standard errors. A pooled estimate was obtained by a random-effects model.¹⁸ We used the package ‘metafor’¹⁷ available for the R language of statistical computing.¹⁶ The work of Daams *et al.*¹⁵ was added later.

Subjects

We obtained MRI scans from 64 HCs and 267 patients with a diagnosis of CIS ($n=85$) or RRMS ($n=182$) according to the 2005 revision of McDonald criteria.²¹ CIS was defined as first demyelinating event suspicious of MS accompanied by at least two MRI-detected brain lesions. Patients did not receive corticosteroid treatment within 30 days prior to MRI scan. The study had been approved by the local ethics committee. Written informed consent was obtained from HCs to undergo an MRI scan for scientific purposes and from patients to provide their MRI scans, acquired in routine clinical practice, for scientific studies. All patients were recruited at the same centre (Klinikum Rechts der Isar, Technische Universität München, Germany).

Disability was quantified using the Expanded Disability Status Scale (EDSS) and in a subgroup of patients by the Fatigue Scale for Motor and Cognitive Functions (FSMC),²² and the Multiple Sclerosis Functional Composite (MSFC) with its three subtests: Nine-Hole Peg Test (9-HPT), Timed 25-Foot Walk (T25-FW) and Paced Auditory Serial Addition Test (PASAT).²³ Exact numbers and main characteristics of the study population are given in Table 1. At MRI acquisition, 126 patients received no disease modifying drug, 85 patients were treated with interferon beta 1a/b, 32 with glatiramer acetate, 21 with natalizumab and three with fingolimod.

MRI

All brain images were acquired on the same 3T scanner (Achieva, Philips, Netherlands). We used a 3D gradient echo (GRE) T1-weighted sequence (orientation, 170

contiguous sagittal 1 mm slices, reaching down to C4/C5; field of view, 240×240 mm; voxel size, 1.0×1.0×1.0 mm; repetition time (TR), 9 ms; echo time (TE), 4 ms), and a 3D fluid attenuated inversion recovery (FLAIR) sequence (orientation, 144 contiguous axial 1.5 mm slices, reaching down to the foramen magnum; field of view, 230×185 mm; voxel size, 1.0×1.0×1.5 mm; TR, 10⁴ ms; TE, 140 ms; TI, 2750 ms).

Spinal cord images, acquired on two different 3T scanners (Achieva, Philips, Netherlands and Verio, Siemens, Germany), were available in a subgroup of patients. The scan protocol included a T1-weighted sequence (orientation, 15 contiguous sagittal 2 mm slices; field of view, 160×250 mm; voxel size, 0.8×1.0×2.0 mm; TR, 524 ms; TE, 8 ms), and a T2-weighted sequence (1. orientation, 15 contiguous sagittal 2 mm slices; field of view, 160×250 mm; voxel size, 0.8×1.07×2.0 mm; TR, 3584 ms; TE, 100 ms; 2. orientation, 82 axial 4 mm slices; field of view 120×120 mm; voxel size, 0.65×0.81×4 mm; TR, 2342 ms; TE, 90 ms).

Measurement of the upper cervical cord area (UCCA)

As described earlier, UCCA was measured from brain MRI covering the upper cervical cord^{24,25} at the level of the C2/C3 intervertebral disc.¹ Measurement of UCCA comprised three steps. First, the original images were manually rotated by the use of commercially available software (Amira 5.3.3, Visage Imaging, Inc.) resulting in vertical orientation of the cervical cord around C2/C3. Second, images were segmented without a priori probability maps into spinal cord parenchyma, including grey matter (GM) plus white matter (WM), and cerebrospinal fluid (CSF) by the use of FSL software (www.fmrib.ox.ac.uk/fsl/). This procedure (‘hard segmentation’) resulted in binary maps. The axial slice at C2/C3 of the corresponding binary map was manually selected. Contiguous voxels of spinal cord parenchyma were automatically counted in the selected slice and multiplied by the voxel size to obtain UCCA in mm². To examine the reliability of our method, UCCA was determined independently by two raters in 267 subjects. Pearson’s correlation coefficient was calculated from the UCCA measurements of the two raters, which showed high agreement ($r=0.975$). To investigate possible systematic deviation between the two measurements, the intercept and slope of the linear function that best describes the relation between the measures of both raters was calculated. The 95% confidence interval was (−0.32–3.6) for the intercept and (0.95–1.01) for the slope. Since the interval for the intercept covers 0 and the interval for the slope

Table 1. Demographic, global imaging and clinical parameters.

	HCs		Patients		<i>p</i> -value HC-Pat	CIS	RRMS	<i>p</i> -value CIS-RRMS
	<i>n</i>		<i>n</i>					
	64		267		–	85	182	–
Age in years (range)	64	35.0 (20–60)	267	35.8 (19–66)	0.663	35.2 (18–58)	36.0 (19–66)	0.563
Gender (male/female)	64	23/41	267	83/185	0.459	28/57	55/127	0.672
Disease duration (years)	64	–	267	3.3±3.9	–	0.8±1.5	4.5±4.2	<0.001
TIV (ml)	64	1387±109	267	1368±136	0.315	1374±127	1366±140	0.624
Volume of cerebral grey matter (ml)	64	859±49	267	837±50	0.002	842±47	835± 52	0.319
Volume of cerebral white matter (ml)	64	683±43	267	667±43	0.007	674±34	663±46	0.031
Volume of cerebral white matter lesions (ml)	64	–	267	3.4±5.7	–	1.9±2.8	4.1±6.5	0.005
UCCA (mm ²)	62	76.1±6.9	239	72.8±6.6	0.001	73.5±5.8	72.4±7.0	0.223
CV of UCCA	58	2.13±0.8	222	2.89±1.3	<0.001	2.38±0.9	3.13±1.4	<0.001
Spinal lesions at C2/C3 (%)	–	–	267	33.7	–	23.5	40.7	0.06
Median EDSS (range)	–	–	267	1.0 (0–5.5)	–	1.0 (0–5.5)	1.5 (0–5.5)	0.008
MSFC	–	–	210	0.57±0.42	–	0.61±0.4	0.54±0.4	0.247
PASAT	–	–	210	46.3±11.1	–	46.6±10.9	46.1±11.2	0.745
T25-FW (s)	–	–	211	4.0±0.9	–	3.8±0.7	4.2±1.0	0.013
9-HPT mean left and right (s)	–	–	211	18.6±2.8	–	18.2±2.4	18.8±3.0	0.157
FSMC	–	–	155	42.9±20.2	–	36.5±18.4	46.0±20.4	0.006
- cognition				20.6±10.1		18.0±9.3	21.9±10.3	0.002
- motor				22.3±10.7		18.6±9.7	24.1±10.8	0.024

CIS: clinically isolated syndrome; CV: coefficient of variation; EDSS: Expanded Disability Status Scale; FSMC: Fatigue Scale for Motor and Cognitive Function; HC: healthy control; MS: multiple sclerosis; MSFC: Multiple Sclerosis Functional Composite; 9-HPT: 9-Hole Peg Test; PASAT: Paced Auditory Serial Addition Test; RRMS: relapsing–remitting multiple sclerosis; T25-FW: Timed 25-Foot Walk; TIV: total intracranial volume; UCCA: upper cervical cord cross-sectional area.

Unpaired *t*-test and Fisher's exact test (gender, presence of spinal lesions) were used to compare groups.

covers 1, there is no evidence for a systematic difference. As MS lesions can influence UCCA by local swelling or shrinking (Figure 1(b)), levels including lesions visible in the T1 image were omitted; instead, UCCA was determined up to 13 mm higher, depending on the size of the lesion. Similarly, levels with poor contrast of the spinal cord to the surrounding CSF were skipped. This approach was justified as we showed earlier in two large cohorts of HCs that the measurement of UCCA between the level of C2/C3 and up to 13 mm above is not influenced by the slice chosen.²⁴ UCCA could not be determined in 28 MS patients and two HCs due to image artefacts or large lesions. Similarly to our earlier findings in HCs,²⁴ we found that UCCA was most strongly correlated with brain WM volume in MS patients ($r=0.333$; $p<0.0001$). UCCA was not correlated with brain T2-hyperintense lesion volume ($p=0.162$).

To quantify the variance in UCC introduced by MS lesions, a coefficient of variation (CV) was calculated from all measurements between the level of C2/C3

and 13 mm higher (standard deviation/mean in %). Levels with and without lesions but not with image artefacts or poor contrast were included; a minimum of eight measurements was required to calculate the CV, resulting in 31 dropouts (four HCs, 27 MS patients).

In a subgroup of 67 patients, simultaneous spinal cord MRI (within 75 days) was available. Visual lesion detection at C2/C3 from brain MRI was compared to visual lesion detection from spinal cord MRI (T1- and T2-weighted, sagittal and transverse plane). In accordance with recent findings,²⁶ the percentage of image artefacts was similar between both methods (brain MRI 4/67, spinal MRI 3/67). Twenty-three lesions were detected with both methods in the same individual; three additional lesions were found with spinal cord MRI, and one additional lesion with brain MRI (which was retrospectively also detected in the spinal cord MRI). Overall, we found that correspondence between both methods was sufficient to justify evaluation of focal lesions from brain MRI.

Analysis of global volumes

T2-hyperintense brain WM lesions were determined by our software package lesion segmentation tool (LST). LST (www.applied-statistics.de/lst.html) includes lesion segmentation in native space²⁷ and lesion filling.²⁸ A natural log transformation (ln) was applied to all lesion volumes to approximate normal distribution.²⁹ Global volumes of GM and WM were derived from the first segmentation step of the VBM8 toolbox (<http://dbm.neuro.uni-jena.de/vbm8>), an extension of SPM8 software (<http://www.fil.ion.ucl.ac.uk/spm>). Total intracranial volume (TIV) was estimated by a 'reverse MNI (Montreal Neurological Institute) brain mask method'.³⁰

Statistical analysis

SPSS 20 and GraphPad Prism 5 were used to analyse and plot data. Group comparisons for demographic, imaging and clinical parameters were assessed by unpaired *t*-test and Fisher's exact test. A two-factorial analysis of variance (ANOVA) was used to assess the effect of the presence of focal lesions (yes/no) and the disease stage (CIS/RRMS) on the CV of UCCA. Correlations of UCCA and the CV of UCCA with imaging and clinical parameters were calculated by simple (Pearson) and partial correlation. Nuisance variables were age, sex, total T2-hyperintense brain WM lesion volume (UCCA and CV of UCCA) and the presence of focal lesions at C2/C3 (CV of UCCA).

The relationship of UCCA and the CV of UCCA with disease duration was estimated in a simple linear regression model. Disease duration was log (lg10) transformed to approximate normality.

Results

Demographic, global imaging and clinical parameters

We analysed structural brain MRI of 64 HCs and 267 patients with RRMS (182; 68%) or CIS (85; 32%). Patients and HCs did not differ in age, gender, and TIV. Compared to HCs, patients had reduced brain GM and WM volumes. Comparing RRMS to CIS patients, we found longer disease duration, reduced brain WM volume, higher T2-hyperintense brain WM lesion volume, more frequent lesions at C2/C3, higher EDSS, slower T25-FW and higher fatigue scores (Table 1).

Structural variability and atrophy of the UCC in early MS

Focal lesions at C2/C3 resulted in higher structural variability, expressed by the CV of UCCA (Figure 2).

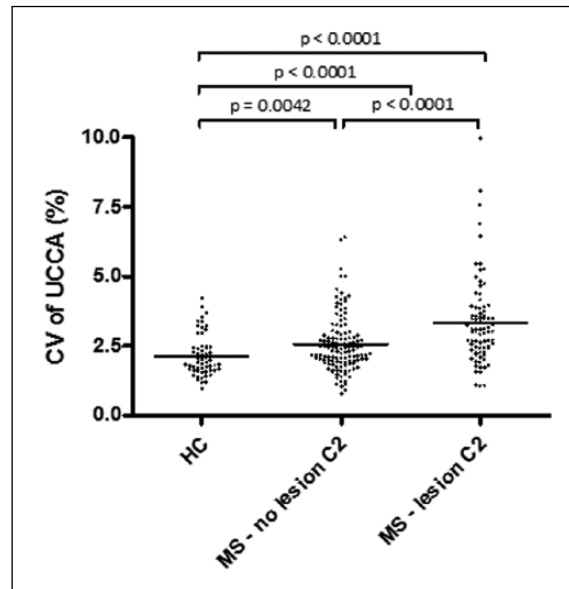


Figure 2. Influence of focal lesions at the group level. Scatter plot of coefficient of variation (CV) of upper cervical cord cross-sectional area (UCCA) is shown separately for healthy controls (HCs) and the subgroups of patients with and without focal lesions. Mean CV of UCCA is marked by a horizontal line. Unpaired *t*-test was performed to compare groups. MS: multiple sclerosis.

However, even in the absence of macroscopic lesions in the UCC, structural variability was higher in MS patients than in HCs. In contrast, UCCA did not differ between patients with and without lesions ($p=0.363$). There was neither a difference between patients with and without disease modifying drugs ($p=0.131$).

Compared to HCs, UCCA was significantly reduced in CIS and RRMS patients, but the difference between both patient groups was not significant (Figure 3(a)). In contrast, the CV of UCCA was significantly higher in RRMS than in CIS (Figure 3(b)). According to the two-factorial ANOVA, this difference was explained by both the higher percentage of focal lesions in RRMS ($p=0.001$) and the disease stage ($p=0.007$). There was a trend towards higher CV of UCCA in CIS patients compared to HCs (Figure 3(b)).

Correlation of spinal cord pathology with clinical parameters

Both markers of spinal cord pathology, UCCA and CV of UCCA, were correlated with disease duration. UCCA and CV of UCCA were also correlated with disease severity assessed by EDSS (Table 2). In addition, the CV of UCCA but not UCCA correlated with 9-HPT and showed a trend towards correlation with motor fatigue.

Table 2. Correlation of spinal cord measures with clinical parameters.

	Disease duration (log 10)	EDSS	MSFC			FSMC	
			T25-FW	Mean 9-HPT	PASAT	Motor	Fatigue
UCCA	-0.134*	-0.131*	n.s.	n.s.	n.s.	n.s.	n.s.
Nuisance variables: age and sex							
CV of UCCA	0.300***	0.192**	n.s.	0.180*	n.s.	0.173	n.s.
Nuisance variables: age and sex						(<i>p</i> =0.052)	
UCCA	-0.132*	-0.129*	n.s.	n.s.	n.s.	n.s.	n.s.
Nuisance variables: age, sex and lesion volume (ln)							
CV of UCCA	0.253***	0.160*	n.s.	0.157*	n.s.	n.s.	n.s.
Nuisance variables: age, sex, lesion volume (ln) and focal lesions C2/C3							

Pearson's correlation coefficients are given. CV: coefficient of variation; EDSS: Expanded Disability Status Scale; FSMC: Fatigue Scale for Motor and Cognitive Functions; 9-HPT: 9-Hole Peg Test; MSFC: Multiple Sclerosis Functional Composite; n.s.: not significant; PASAT: Paced Auditory Serial Addition Test; T25-FW: Timed 25-Foot Walk; TIV: total intracranial volume; UCCA: upper cervical cord cross-sectional area.
p*<0.05; *p*<0.01; ****p*<0.001.

Correlation of UCCA with disease duration and EDSS survived correction for total T2-hyperintense lesion volume. Significant correlations of the CV of UCCA with disease duration, EDSS and 9-HPT persisted after correction for both total T2-hyperintense brain WM lesion volume and presence of focal lesions.

Discussion

This cross-sectional study was conducted to determine the onset of spinal cord atrophy in the disease course of MS and disentangle conflicting results of previous studies. We identified focal MS lesions as potential confounder. Accounting for this finding, we investigated UCCA in a large cohort of CIS and RRMS patients and found significant atrophy in both patient groups compared to HCs. Structural variability of UCC was higher in MS, which was in part, but not completely, explained by focal lesions. Atrophy of the spinal cord, and even more its variability, explained differences in clinical disability even after adjustment for T2-hyperintense brain WM lesion volume, which is the most established measure of brain pathology in MS.³¹ In the following, we will discuss the influence of focal lesions on spinal cord atrophy, speculate on the nature of increased structural variability of UCC, consider the potential of UCC measures with regard to clinical practice and research, acknowledge limitations of our study and relate our findings to the current literature.

We could demonstrate at the group level that focal lesions add variance to UCC measures. This is in line with earlier reports^{19,20,32} and with our single case

observations that macroscopically visible focal WM lesions can cause either local swelling or shrinking (Figure 1(b)). In our cohort, the presence of focal lesions increased the CV of UCCA but did not affect UCCA itself indicating that both effects, swelling and shrinking, were present but counterbalanced in our cohort. However, lesions might introduce a systematic bias in other cohorts, which is conceivable given the commonly held view that swelling is caused by acute inflammatory lesions and shrinking by chronic lesions. Consequently, to account for focal lesions is warranted for evaluation of spinal cord atrophy in early MS in order to reduce variance and not to overestimate (in case of shrunken lesion) or miss (in case of swelled lesion) an effect.

Intriguingly, we observed that variability of UCC was higher in MS even in the absence of macroscopic lesions, which may simply result from invisible or diffuse lesions. Alternatively, the CV of UCCA might cover at least one component of structural variability independent of focal lesions. Since the CV of UCCA correlated more strongly with disease duration and clinical parameters than UCCA itself, even after correction for the presence of focal lesions, it is unlikely that this component constitutes an epiphenomenon. Yet we can only speculate on its nature. Atrophy may develop unequally in a scattered manner, which could lead to increased variability of UCCA across contiguous levels before a decrease in UCCA becomes apparent. Alternatively, more subtle damage from widespread MS pathology in UCC may induce variance in UCCA measures. Indeed, evidence from more sophisticated

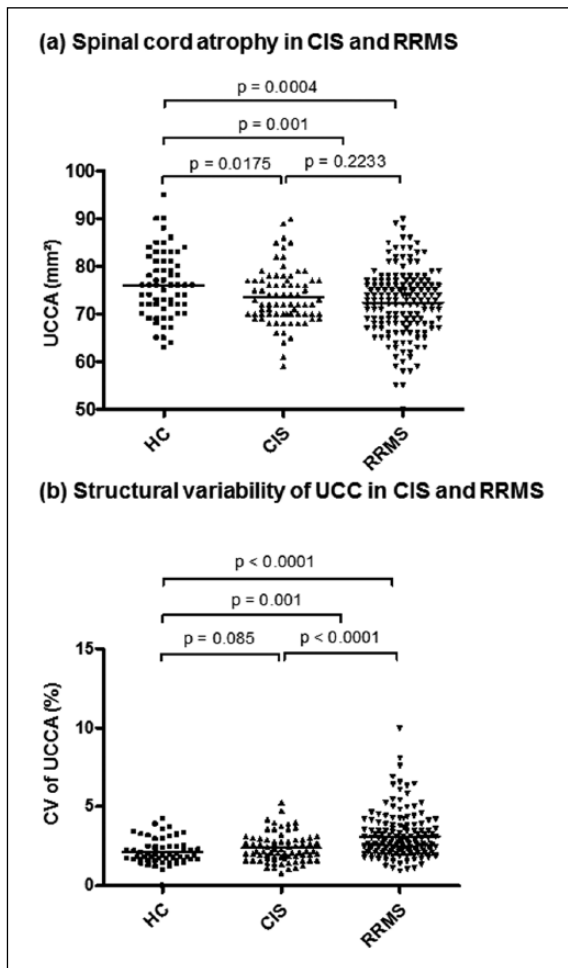


Figure 3. Group comparison of spinal cord measures. (a) Spinal cord atrophy in clinically isolated syndrome (CIS) and relapsing–remitting multiple sclerosis (RRMS). Scatter diagram of upper cervical cord cross-sectional area (UCCA) for healthy controls (HCs), CIS and RRMS is shown. Mean UCCA is marked by a horizontal line. Unpaired *t*-test was performed to compare groups. (b) Structural variability of upper cervical cord (UCC) in CIS and RRMS. Scatter diagram of coefficient of variation (CV) of UCCA for HCs, CIS and RRMS is shown. Mean CV of UCCA is marked by a horizontal line. Unpaired *t*-test was performed to compare groups.

MRI methods such as texture analysis³³ or quantitative MRI^{34–36} points towards the existence of those microscopic structural changes in the cervical cord in MS and their association with clinical disability^{33,34,36} before UCCA decreases.³³ Pial and subpial abnormalities of cervical spinal cord in MS, as suggested recently based on a magnetisation transfer ratio,³⁷ might also contribute to our measure of structural variability.

Both parameters of spinal cord pathology, UCCA and CV of UCCA, are of value to describe and potentially monitor MS because of their correlation with disease duration after correction for T2-hyperintense brain

WM lesion volume. Correlations of UCCA with clinical parameters given in Table 2 did not survive adjustment for brain atrophy, whereas correlations of CV of UCCA did. This might be explained by the fact that UCCA and brain volume are not only changed in MS but also strongly correlated in HCs, as we demonstrated recently,²⁴ so that including brain atrophy as a nuisance variable, when assessing correlations of UCCA, could introduce collinearity into the model and produce false negative results. We acknowledge that we were unable to disentangle the effect of brain and spinal cord atrophy.

Although significant, the correlation of UCCA with EDSS was rather weak in contrast to previous studies,^{2,4,15,32} which might be due to the low EDSS score and, hence, the small range of disease severity covered by our group (Table 1). The measure of variability in contrast, correlated better with clinical disability. In addition to EDSS, it was correlated with hand and arm function and showed a trend to correlation with motor fatigue. The latter is in line with previous findings of a relationship between an abnormal cervical cord function and motor fatigue in MS.³⁸ Correlations between the CV of UCCA and clinical parameters remained significant even after correction for the presence of focal lesions and T2-hyperintense brain WM lesions, indicating that subtle changes, not detectable with the naked eye in conventional MRI mediate this relation.

We acknowledge some limitations of our study. UCCA could not be determined in 28 out of 267 patients. For most of them (22/28), this was due to large lesions in the area of the measurement that could not be omitted. Only six patients and two HCs had to be excluded because of image artefacts. Dropout rates for the CV of UCCA were similar (27 MS, four HCs). Drop out and artefact rate was higher in the CIS/MS group which might bias the results. Clinical tests other than EDSS were only performed in 60–80% of the patients, limiting the comparability of the estimated correlations. Furthermore, the CV of UCCA is a simple but also limited parameter to determine structural variability in the spinal cord and the potential of this parameter needs to be further determined in future studies. Finally, although our results are well compatible with our hypothesis that the disregard of focal lesions may have caused the conflicting results of former studies,^{2,3,8–15} we did not address this issue directly. It is also conceivable that, besides focal spinal cord lesions, other factors such as smaller sample sizes (Figure 1(a)) or different methodological approaches (e.g. planimetric vs volumetric measurements, different image resolutions, different MRI

field strengths) or a combination thereof may have resulted in the heterogeneous results of former studies. Not unexpectedly, repetition of our meta-analysis after inclusion of our data did not yield significant overall results neither with regard to RRMS nor with regard to CIS, although a trend to spinal cord atrophy in RRMS was observed. Thus from a conservative point of view, our findings require replication by a study of a similarly large cohort with a methodology accounting for focal lesions.

In conclusion, we could demonstrate in a large cohort that spinal cord atrophy is present in MS patients as early as in CIS and is associated with clinical disability. Structural variability in the spinal cord cannot fully be explained by focal lesions but may be a more meaningful marker of spinal cord pathology in early MS than spinal cord atrophy.

Conflict of interest

Viola Biberacher received research support from Merck Serono.

Dorothea Buck has received compensation for activities with Bayer-Healthcare, BiogenIdec, Merck-Serono, and Novartis. She was supported by the Commission for Clinical Research of the Faculty of Medicine, TU München, the Anti-Biopharmaceutical Immunization: prediction and analysis of clinical relevance to minimize the RISK (ABIRISK) programme, and the Progressive Multifocal Leukoencephalopathy Consortium(PML).

Muna-Miriam Hoshi has received compensation for activities with Bayer Health Care, Biogen Idec, Merck Serono, Novartis.

Achim Berthele is a consultant for Biogen Idec, Bayer, Merck Serono; he has received research support from Bayer; he has received honoraria for lecturing from Biogen Idec, Bayer, Merck Serono, Teva Neuroscience, Novartis; he has received travel expenses for attending meetings from Biogen Idec, Merck Serono, Bayer, Teva Neuroscience, Novartis; he has received Investigator fees for Phase II-IV clinical studies from Biogen Idec, Novartis, Merck Serono, and Galapagos.

Bernhard Hemmer served on scientific advisory boards and/or as a consultant for Roche, Biogen Idec, Bayer, Novartis, GSK, Chugai and Merck Serono; he has received research support from Novartis, Merck Serono, Biogen Idec, Roche, Chugai, 5-Prime, metanomics and Bayer; he has received honoraria for lecturing from Teva Neuroscience, BiogenIdec, Bayer, Novartis, Merck Serono, Roche; he has received travel expenses for attending meetings from Roche, Teva Neuroscience, Biogen Idec, Bayer, Novartis, Merck Serono.

Mark Mühlau has received research support from Merck Serono and Novartis; he has received travel expenses for attending meetings from Bayer, and Merck Serono.

Christine C Boucard, Paul Schmidt, Christina Engl and Claus Zimmer have nothing to disclose.

Funding

This work was supported by Merck Serono, and the 'German Competence Network Multiple Sclerosis' (KKNMS).

References

1. Losseff NA, Webb SL, O'Riordan JI, et al. Spinal cord atrophy and disability in multiple sclerosis. A new reproducible and sensitive MRI method with potential to monitor disease progression. *Brain* 1996; 119: 701–708.
2. Rocca MA, Horsfield MA, Sala S, et al. A multicenter assessment of cervical cord atrophy among MS clinical phenotypes. *Neurology* 2011; 76: 2096–2102.
3. Liu C, Edwards S, Gong Q, et al. Three dimensional MRI estimates of brain and spinal cord atrophy in multiple sclerosis. *J Neurol Neurosurg Psychiatry* 1999; 66: 323–330.
4. Furby J, Hayton T, Anderson V, et al. Magnetic resonance imaging measures of brain and spinal cord atrophy correlate with clinical impairment in secondary progressive multiple sclerosis. *Mult Scler* 2008; 14: 1068–1075.
5. Furby J, Hayton T, Altmann D, et al. A longitudinal study of MRI-detected atrophy in secondary progressive multiple sclerosis. *J Neurol* 2010; 257: 1508–1516.
6. Stevenson VL, Leary SM, Losseff NA, et al. Spinal cord atrophy and disability in MS: A longitudinal study. *Neurology* 1998; 51: 234–238.
7. Filippi M, Campi A, Colombo B, et al. A spinal cord MRI study of benign and secondary progressive multiple sclerosis. *J Neurol* 1996; 243: 502–505.
8. Lin X, Blumhardt LD and Constantinescu CS. The relationship of brain and cervical cord volume to disability in clinical subtypes of multiple sclerosis: A three-dimensional MRI study. *Acta Neurol Scand* 2003; 108: 401–406.
9. Brex PA, Leary SM, O'Riordan JI, et al. Measurement of spinal cord area in clinically isolated syndromes suggestive of multiple sclerosis. *J Neurol Neurosurg Psychiatry* 2001; 70: 544–547.
10. Mann RS, Constantinescu CS and Tench CR. Upper cervical spinal cord cross-sectional area in relapsing

- remitting multiple sclerosis: Application of a new technique for measuring cross-sectional area on magnetic resonance images. *J Magn Reson Imaging* 2007; 26: 61–65.
11. Rashid W, Davies GR, Chard DT, et al. Upper cervical cord area in early relapsing-remitting multiple sclerosis: Cross-sectional study of factors influencing cord size. *J Magn Reson Imaging* 2006; 23: 473–476.
 12. Rashid W, Davies GR, Chard DT, et al. Increasing cord atrophy in early relapsing-remitting multiple sclerosis: A 3 year study. *J Neurol Neurosurg Psychiatry* 2006; 77: 51–55.
 13. Rocca MA, Valsasina P, Damjanovic D, et al. Voxel-wise mapping of cervical cord damage in multiple sclerosis patients with different clinical phenotypes. *J Neurol Neurosurg Psychiatry* 2013; 84: 35–41.
 14. Zivadinov R, Banas AC, Yella V, et al. Comparison of three different methods for measurement of cervical cord atrophy in multiple sclerosis. *AJNR Am J Neuroradiol* 2008; 29: 319–325.
 15. Daams M, Weiler F, Steenwijk MD, et al. Mean upper cervical cord area (MUCCA) measurement in long-standing multiple sclerosis: Relation to brain findings and clinical disability. *Mult Scler* [Epub ahead of print: DOI 10.1177/1352458514533399].
 16. R Core Team. *R: A language and environment for statistical computing*. Vienna, Austria: R Foundation for Statistical Computing, 2013.
 17. Viechtbauer W. Conducting meta-analyses in R with the metafor package. *J Stat Softw* 2010; 36: 1–48.
 18. Viechtbauer W. Bias and efficiency of meta-analytic variance estimators in the random-effects model. *J Educ Behav Stat* 2005; 30: 261–293.
 19. Evangelou N, DeLuca GC, Owens T, et al. Pathological study of spinal cord atrophy in multiple sclerosis suggests limited role of local lesions. *Brain* 2005; 128: 29–34.
 20. Rocca MA, Mastronardo G, Horsfield MA, et al. Comparison of three MR sequences for the detection of cervical cord lesions in patients with multiple sclerosis. *AJNR Am J Neuroradiol* 1999; 20: 1710–1716.
 21. Polman CH, Reingold SC, Edan G, et al. Diagnostic criteria for multiple sclerosis: 2005 Revisions to the ‘McDonald Criteria’. *Ann Neurol* 2005; 58: 840–846.
 22. Penner IK, Raselli C, Stocklin M, et al. The Fatigue Scale for Motor and Cognitive Functions (FSMC): Validation of a new instrument to assess multiple sclerosis-related fatigue. *Mult Scler* 2009; 15: 1509–1517.
 23. Cutter GR, Baier ML, Rudick RA, et al. Development of a multiple sclerosis functional composite as a clinical trial outcome measure. *Brain* 1999; 122: 871–882.
 24. Engl C, Schmidt P, Arsic M, et al. Brain size and white matter content of cerebrospinal tracts determine the upper cervical cord area: Evidence from structural brain MRI. *Neuroradiology* 2013; 55: 963–970.
 25. Freund PA, Dalton C, Wheeler-Kingshott CA, et al. Method for simultaneous voxel-based morphometry of the brain and cervical spinal cord area measurements using 3D-MDEFT. *J Magn Reson Imaging* 2010; 32: 1242–1247.
 26. Nair G, Absinta M and Reich DS. Optimized T1-MPRAGE sequence for better visualization of spinal cord multiple sclerosis lesions at 3T. *AJNR Am J Neuroradiol* 2013; 34: 2215–2222.
 27. Schmidt P, Gaser C, Arsic M, et al. An automated tool for detection of FLAIR-hyperintense white-matter lesions in multiple sclerosis. *Neuroimage* 2012; 59: 3774–3783.
 28. Chard DT, Jackson JS, Miller DH, et al. Reducing the impact of white matter lesions on automated measures of brain gray and white matter volumes. *J Magn Reson Imaging* 2010; 32: 223–228.
 29. Gourraud PA, Sdika M, Khankhanian P, et al. A genome-wide association study of brain lesion distribution in multiple sclerosis. *Brain* 2013; 136: 1012–1024.
 30. Keihaninejad S, Heckemann RA, Fagiolo G, et al. A robust method to estimate the intracranial volume across MRI field strengths (1.5T and 3T). *Neuroimage* 2010; 50: 1427–1437.
 31. Sormani MP and Bruzzi P. MRI lesions as a surrogate for relapses in multiple sclerosis: A meta-analysis of randomised trials. *Lancet Neurol* 2013; 12: 669–676.
 32. Lukas C, Sombekke MH, Bellenberg B, et al. Relevance of spinal cord abnormalities to clinical disability in multiple sclerosis: MR imaging findings in a large cohort of patients. *Radiology* 2013; 269: 542–552.
 33. Mathias JM, Tofts PS and Losseff NA. Texture analysis of spinal cord pathology in multiple sclerosis. *Magn Reson Med* 1999; 42: 929–935.
 34. Oh J, Saidha S, Chen M, et al. Spinal cord quantitative MRI discriminates between disability levels in multiple sclerosis. *Neurology* 2013; 80: 540–547.
 35. Raz E, Bester M, Sigmund EE, et al. A better characterization of spinal cord damage in multiple sclerosis: A diffusional kurtosis imaging study. *AJNR Am J Neuroradiol* 2013; 34: 1846–1852.

Visit SAGE journals online
<http://msj.sagepub.com>

 SAGE journals

36. Naismith RT, Xu J, Klawiter EC, et al. Spinal cord tract diffusion tensor imaging reveals disability substrate in demyelinating disease. *Neurology* 2013; 80: 2201–2209.
37. Kearney H, Yiannakas MC, Samson RS, et al. Investigation of magnetization transfer ratio-derived pial and subpial abnormalities in the multiple sclerosis spinal cord. *Brain* [Epub ahead of print: doi: 10.1093/brain/awu171].
38. Rocca MA, Absinta M, Valsasina P, et al. Abnormal cervical cord function contributes to fatigue in multiple sclerosis. *Mult Scler* 2012; 18: 1552–1559.